Received: 1 December 2021 | Revised: 21 January 2022 | Accepted: 11 March 2022

DOI: 10.1002/lio2.785

ORIGINAL RESEARCH

Laryngoscope Investigative Otolaryngology

Analysis of the epidermal growth factor receptor/phosphoinositide-dependent protein kinase-1 axis in tumor of the external auditory canal in response to epidermal growth factor stimulation

Naotaro Akiyama MD, PhD[1] | Tomomi Yamamoto-Fukuda MD, PhD[2] | Mamoru Yoshikawa MD, PhD[1] | Hiromi Kojima MD, PhD[2]

[1]Department of Otorhinolaryngology, Toho University School of Medicine, Tokyo, Japan

[2]Department of Otorhinolaryngology, Jikei University School of Medicine, Tokyo, Japan

Correspondence
Naotaro Akiyama, Department of Otorhinolaryngology, Toho University School of Medicine, 2-22-36, Ohashi, Meguro-ku, Tokyo 153-8515, Japan.
Email: naotaro.akiyama@med.toho-u.ac.jp

Tomomi Yamamoto-Fukuda, Department of Otorhinolaryngology, Jikei University School of Medicine, 3-25-8, Nishishinbashi, Minato-ku, Tokyo 105-8461, Japan.
Email: tomomiyf@jikei.ac.jp

Funding information
This study is supported by a Grant-in-Aid for Scientific Research from the Japanese Society for the Promotor of Science (JSPS) (no. JP16K11186 and JP19K09857 to T. Yamamoto-Fukuda, no. JP18K16908 to N. Akiyama).

Abstract

Objectives: The epidermal growth factor receptor (EGFR) is related to the invasion and metastasis of external auditory canal (EAC) squamous cell carcinoma (SCC). The phosphoinositide-dependent protein kinase-1 (PDPK1) accelerates tumor cell growth through anti-apoptotic signaling under the influence of downstream EGFR-mediated signaling pathways. In this study, we investigated the EGFR/PDPK1 axis in the EAC under EGF stimulation.

Methods: We confirmed EGFR and PDPK1 expression in human EACSCC specimens immunohistochemically. We next transfected the EGF expression vector in the mouse EAC and then conducted a PDPK1 inhibitory experiment. Immunohistochemical analysis was performed in the mouse EAC, using anti-EGF, anti-EGFR, anti-PDPK1, and anti-Ki67 antibodies. Immunohistochemical analysis of cleaved caspase-3 and terminal deoxy(d)-UTP nick end labeling (TUNEL) detection assays were also performed for the assessment of apoptosis in the inhibitory experiment.

Results: Immunohistochemical analysis revealed overexpression and colocalization of EGFR and PDPK1 in human EACSCC specimens. The growth of a protuberant tumor was observed in the mouse EAC in which EGF expression vector was transfected, and EGF, EGFR, PDPK1, and Ki67 labeling indexes (LIs) were significantly increased. PDPK1 inhibition then induced normal epithelial appearance in the EAC. Moreover, EGF, EGFR, PDPK1, and Ki67 LIs were decreased, and cleaved caspase-3 and TUNEL LIs were increased in the EAC.

Conclusion: We demonstrated the possibility that PDPK1 plays an important role in EACSCC.

Level of Evidence: NA.

KEYWORDS
EGFR, external auditory canal squamous cell carcinoma, PDPK1

1 | INTRODUCTION

Carcinoma of the external auditory canal (EAC) is a rare disease, representing 1–5 cases per million people per year.[1–5] Squamous cell carcinoma (SCC) is the most common histologic type of this disease. The pathogenesis of EACSCC is not fully understood because of the rarity of this disease. EACSCC is locally aggressive due to the anatomical features of the temporal bone which facilitates tumor spread via microscopic diffusion through the bony canals as well as nerve and intraosseous vessels.[2–6] Surgical resection with or without adjuvant radiotherapy is the main strategy for EACSCC.[1–5] Although the prognosis for patients has been improved by advances in surgery and multidrug chemoradiotherapy, it is still poor in the advanced stages.[2,5–8]

The epidermal growth factor receptor (EGFR) belongs to the ErbB family of receptor tyrosine kinases and is activated following its binding with peptide growth factors of the EGF family.[9] Activated EGFR is involved in the pathogenesis and progression of EACSCC[10,11] the same as in head and neck SCC (HNSCC).[9,12–14] Several anti-EGFR therapeutic strategies have been developed in HNSCC, targeting the extracellular or intracellular domain of the EGFR.[15,16] However, the efficacy of these drugs is still limited because of intrinsic and acquired drug resistance, which is mainly due to tumor heterogeneity and genetic instability.[15–18] In addition to the direct activation of EGFR by ligands, EGFR can be transactivated by G protein-coupled receptors mediated by phosphoinositide 3-kinase (PI3K),[19,20] and activating alterations to the PI3K-signaling pathway are observed in HNSCC.[14] Recently, Basura et al. screened gene mutation profiles of EACSCC and reported recurrent alterations of EGFR and PI3K.[11] Phosphoinositide-dependent protein kinase (PDPK1) is a downstream target of PI3K and plays a critical role in the tumor cell migration and invasion of many cancer cells, including HNSCC cells, and is expected to be a new therapeutic target for HNSCC.[21–23]

In this study, we demonstrated the immunohistochemistry of EGFR and PDPK1 in human EACSCC specimens. We then transfected the EGF expression vector in the mouse EAC and analyzed the EGFR/PDPK1 axis immunohistochemically. We also conducted inhibitory experiments targeting to PDPK1 by systemic administration of the PDPK1 inhibitor in this model.

2 | MATERIALS AND METHODS

2.1 | Patients, specimen harvest, and tissue preparation

Between February 2009 and May 2021, 10 patients (4 males and 6 females; age range 35–83 years [y]; mean age 53 y) with EACSCC were treated surgically at the Department of Otorhinolaryngology, Jikei University Hospital. All of the EACSCC tissue samples harvested from the patients during surgery were diagnosed by histopathologic examination. This study protocol was approved by the Human Ethics Review Committee of the Jikei University School of Medicine and signed informed consent was obtained from all of the patients or their guardians for this study (approval number 31-139 9638). Samples were fixed, embedded in paraffin, and 5-μm thick serial sections were prepared in the standard manner.[24] For the histological examination, hematoxylin and eosin (H&E) staining was performed using a standard procedure.

2.2 | Animals

The experiments were conducted in 14 male BALB/c mice (6 weeks, 30–35 g) with a normal tympanic membrane (TM). The animal care and experimental procedures were performed in accordance with the Guidelines for Animal Experimentation of Jikei University with approval guidelines (No. 2015-139C5).

2.3 | Electroporatical transfection of hEGF-expression vector to the mice ears

The 3X FLAG human (h) full-length EGF vector was constructed by inserting the cDNA to the p3xFLAG-CMV14 vector (Sigma Chemical Co., Saint Louis, MO). Flag-h EGF DNA plasmid driven by a CMV14 promoter (0.5 μg/ml) (EGF-expression vector) was transfected once ($n = 2$, 4 ears) or five times every fourth day into the epithelial region of the mouse ear canals ($n = 12$, 12 ears) using a Nepa21 Electroporator (Nepa Gene Co., Chiba, Japan) under anesthesia using a combination anesthetic (0.3 mg/kg of medetomidine, 4.0 mg/kg of midazolam, and 5.0 mg/kg of butorphanol), according to the protocol of a previous study.[25] As a control, a null plasmid driven by a CMV14 promoter (0.5 μg/ml) (empty vector) was transfected into the other ears ($n = 12$, 12 ears) of the mice.[25]

2.4 | Otoendoscopic examination

At every time-point after the EGF-expression vector or empty vector transfection and after PDPK1 inhibitor GSK2334470 (Cayman Chemical, Ann Arbor, MI) administration, an otoendoscopic examination was performed with a rigid rod 0° otoendoscope (AVS Co., Tokyo, Japan) under anesthesia.[25]

2.5 | Administration of PDPK1 inhibitor GSK2334470 in vivo

EGF-expression vector was transfected five times every fourth day into the epithelial region of the right EAC ($n = 8$, 8 ears) and empty vector was transfected five times in the left EAC as control in mice ($n = 8$, 8 ears). After confirming tumor formation in the right EAC by otoendoscopy, PDPK1 inhibitor GSK2334470 (40 mg/kg/day) or phosphate-buffered saline (PBS) ($n = 4$, each) was administered intraperitoneally for five consecutive days.[26]

2.6 | Tissue preparation of the animal model

The mice were euthanized using an intraperitoneal injection of 200 mg/kg pentobarbital and their ears and temporal bones were removed and fixed with 4% paraformaldehyde in PBS at 4°C overnight. The ears were embedded in paraffin and 5 μm serial sections were prepared in a standard manner.[27,28] The temporal bones were decalcified by 10% ethylenediaminetetraacetic acid (EDTA) at 4°C for 7 days and paraffin sections were prepared as described previously.[24,29]

2.7 | Immunohistochemistry

Immunohistochemistry was performed with the indirect enzyme-labeled antibody method, as described previously.[30–33] In brief, after deparaffinization and rehydration, the sections were autoclaved in a Tris-EDTA buffer (pH 9.0) at 120°C for 10 min to detect cleaved caspase-3, a 0.01 M citrate buffer (pH 6.0) at 90°C for 20 min to detect EGFR (A-10) and PDPK1 (EP569Y), or in the HistoVT one (Nacalai Tesque, Kyoto, Japan) at 90°C for 20 min to detect FLAG, Ki67, EGF, EGFR (EP38Y), and PDPK1 (E3). They were preincubated with 500 μg/ml normal goat IgG in 1% bovine serum albumin (Sigma) in PBS for 60 min to block a nonspecific reaction and treated with the first antibodies (Table 1) overnight. After washing the slides with 0.05% Tween 20 in PBS, the slides were reacted with the secondary antibodies listed in Table 1, and washed with 0.05% Tween 20 in PBS. For visualization, 3,3′-diaminobenzidine-4HCl in H_2O_2 was used for the horseradish peroxidase sites, or fluorescence conjugate was used for fluorescent staining. The slides were counterstained with hematoxylin or 4′,6-diamidino-2-phenylindole (DAPI). As a negative control, normal mouse IgG (1:100) or normal rabbit IgG (1:100) was used instead of the first antibodies, respectively, in every experiment.

2.8 | Terminal deoxy(d)-UTP nick end labeling

For terminal deoxy(d)-UTP nick end labeling (TUNEL) detection, an In Situ Cell Death Detection Kit, fluorescein (Roche Applied Science, Penzberg, Germany) was used. The sections were immersed in 0.2 mol/ml proteinase K (Dako, Santa Clara, CA) in PBS at 37°C in a water bath after deparaffinization. The TUNEL reaction mixture was then added to the samples and the slides were incubated for 60 min at 37°C in accordance with the manufacturer's instructions. After being washed with PBS, the slides were counterstained with DAPI.

2.9 | Microscopy, image analysis, and statistical analysis

Bright-field images were obtained using a Zeiss microscope and fluorescent images were obtained using a Zeiss LSM 880 confocal laser scanning microscope connected to a CCD camera (AxioCam, Carl Zeiss, Jena, Germany). Image analysis was performed using Zeiss acquisition analysis software (Zen 2.1 black edition). For each section, more than 1000 cell nuclei were counted in three equal epithelial or stromal regions at 400× magnification in bright-field images or three 10,000 μm^2 areas (100 × 100 μm^2) in fluorescent images. The number of positive cells was expressed as a percentage of positive cells per total number of counted cells, respectively (labeling index [LI]; mean ± standard deviation). The thickness of the epithelium was measured at four locations (central and at each extreme) using NIH Image/ImageJ software as described previously (ver. 1.46r).[34] Differences between the groups were examined for statistical significance using the one-way analysis of variance test followed by the unpaired *t*-test. A *p*-value of less than .05 denoted a statistically significant difference. All analyses were performed using a statistical software package (JMP version 13; SAS Institute Japan, Tokyo, Japan).

TABLE 1 Antibodies used for immunostaining

Antigen, clone name, or immunogen	Manufacturer, species, catalog no.	Dilution used	Type
FLAG, M2	Sigma-Aldrich, St. Louis, MO, mouse, F1804	1:500	Primary
Ki67, mouse KI67 aa.1850-1950	Novus Biologicals, Centennial, CO, rabbit, NB110-89717	1:400	Primary
EGF, 90-140/208	Bioss Antibodies, Woburn, MA, rabbit, bs-3576R	1:200	Primary
EGFR, A-10	Santa Cruz Biotechnology, Dallas, TX, mouse, sc-373746	1:50	Primary
EGFR, EP38Y	Abcam, Cambridge, UK, rabbit, ab52894	1:100	Primary
PDPK1, E3	Santa Cruz Biotechnology, Dallas, TX, mouse, sc-17765	1:100	Primary
PDPK1, EP569Y	Abcam, Cambridge, UK, rabbit, ab52893	1:150	Primary
Cleaved caspase-3, Asp175	Cell signaling Technology, Danvers, MA, rabbit, #9661	1:200	Primary
HRP-goat anti-mouse IgG	Abcam, Cambridge, UK, goat, ab6789	1:100	Secondary
HRP-goat anti-rabbit IgG	Abcam, Cambridge, UK, goat, ab6721	1:100	Secondary
Alexa Fluor 488-goat anti-mouse IgG	Thermo Fisher Scientific, Hudson, NH, goat, A-11008	1:500	Secondary
Alexa Fluor 555-goat anti-rabbit IgG	Thermo Fisher Scientific, Hudson, NH, goat, A-21422	1:500	Secondary

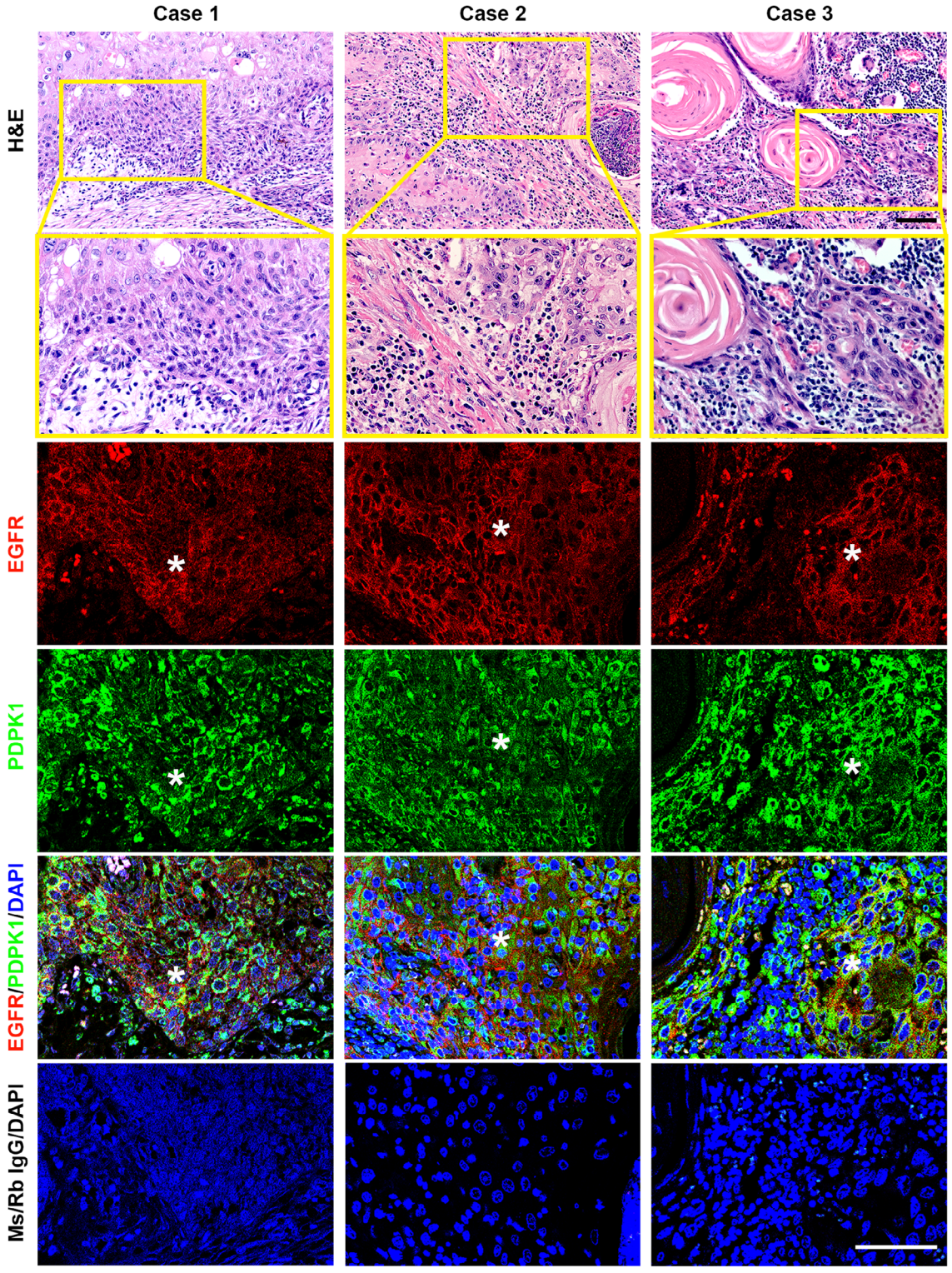

FIGURE 1 Analysis of human squamous cell carcinoma (SCC) of the external auditory canal (EAC). Representative images of hematoxylin and eosin (H&E) stainings of human EACSCC. Squamous cells arising from the epidermis and extending into the dermis exhibiting architectural abnormalities, cytological atypia, and chromatin condensation. The yellow-boxed area is shown in the immunofluorescence stainings. EGFR-positive (+) cells were mainly observed in the lower layers of the epidermis. In the double immunofluorescence staining of EGFR (red) and PDPK1 (green), EGFR+/PDPK1+ cells were mainly observed in the lower layers of the epidermis (asterisks). Negative control was obtained by normal mouse (Ms) IgG and normal rabbit (Rb) IgG instead of first antibodies. The nuclei were stained with DAPI (blue). Scale bars: 100 μm

3 | RESULTS

3.1 | Localization of EGFR- and PDPK1-positive cells in human EACSCC tissues

Representative H&E stainings of the human EACSCC specimen are shown in Figure 1. Squamous cells were noted arising from the epidermis and extending into the dermis, exhibiting architectural abnormalities, cytological atypia, and chromatin condensation (Figure 1, yellow-boxed area).[2,35] EGFR and PDPK1-positive (+) cells were detected in all tissues (10/10, 100%). In the double immunofluorescent staining of EGFR and PDPK1, EGFR+/PDPK1+ cells were almost found to colocalize in the epidermis (Figure 1). No staining was detected with normal mouse IgG and normal rabbit IgG instead of with the first antibody (Figure 1).

3.2 | Evaluation of the EGF-expression vector-transfected ears

Flag protein and EGF-expression were detected immunohistochemically in almost all epithelial cells and some stromal cells in the sections of the

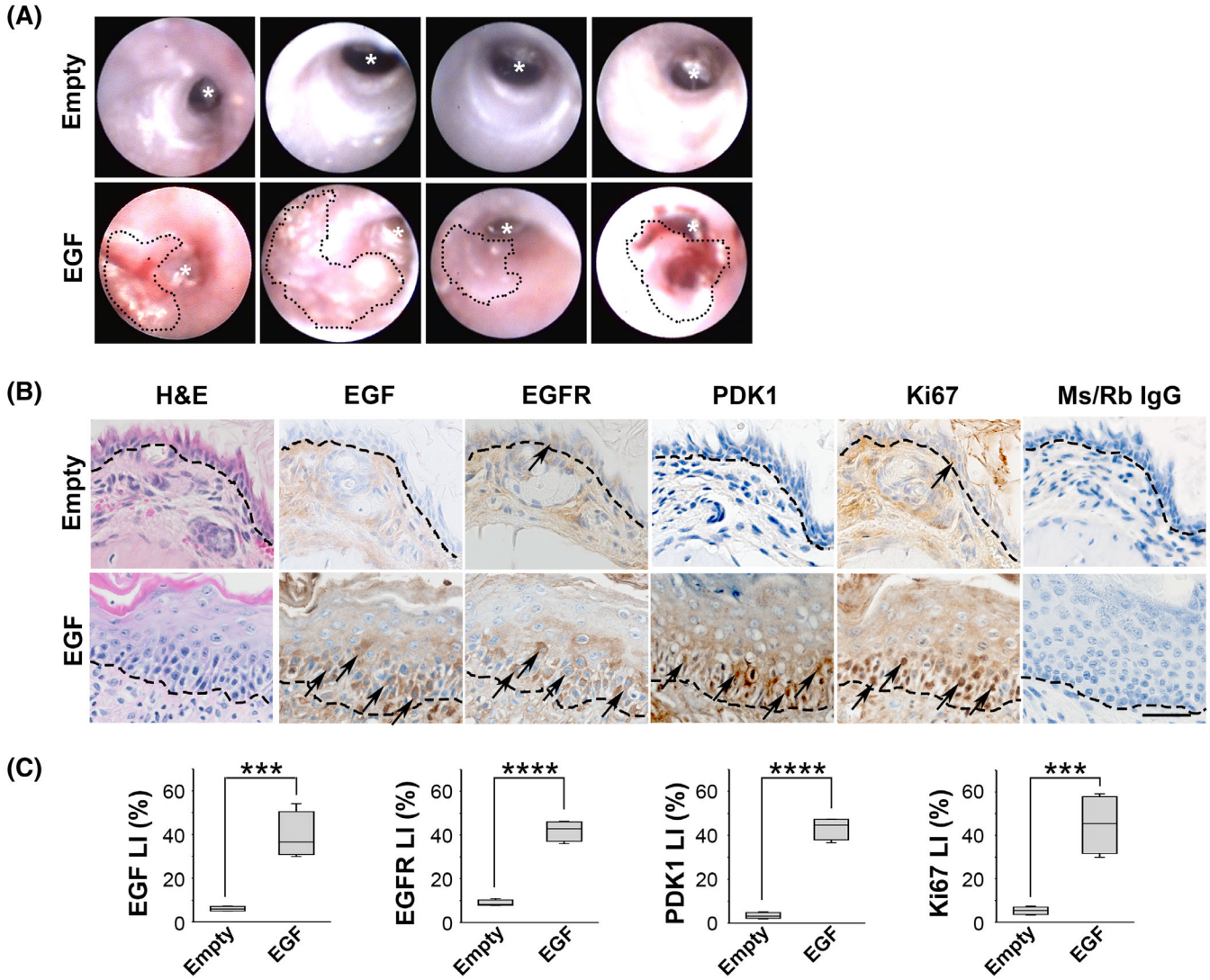

FIGURE 2 Evaluation of the mouse external auditory canal (EAC) into which EGF-expression vector was transfected. (A) Otoendoscopic views of empty or EGF-expression vector-transfected ears. The area within the dotted lines indicates the region of protuberant tumor formation in the EAC in which the EGF-expression vector was transfected. (B) Morphological and immunohistochemical analysis of empty or EGF-expression vector-transfected ears. Hematoxylin and eosin (H&E) staining revealed a thickened epithelium of the EAC into which EGF-expression vector was transfected, while a normal appearance was observed in the EAC into which empty vector was transfected. Immunohistochemical analysis revealed EGF-positive (+)/EGFR+/PDPK1+ cells were detected in the lower layers of the thickened epithelium of the EGF group. Ki67+ cells were also detected in the EGF+/EGFR+/PDPK1+ layers in the section of the EGF group. Negative control was obtained by normal mouse (Ms) IgG and normal rabbit (Rb) IgG instead of first antibodies. (C) Labeling indexes (LIs) of EGF, EGFR, PDPK1, and Ki67 in the epithelium of the EAC in which empty, or EGF-expression vector was transfected ($n = 4$, each). Asterisks: tympanic membrane. Dashed lines: basement membrane. Arrows: positive cells. Scale bar: 20 μm. Error bars: 95% confidence interval. ***p <.001, ****p <.0001

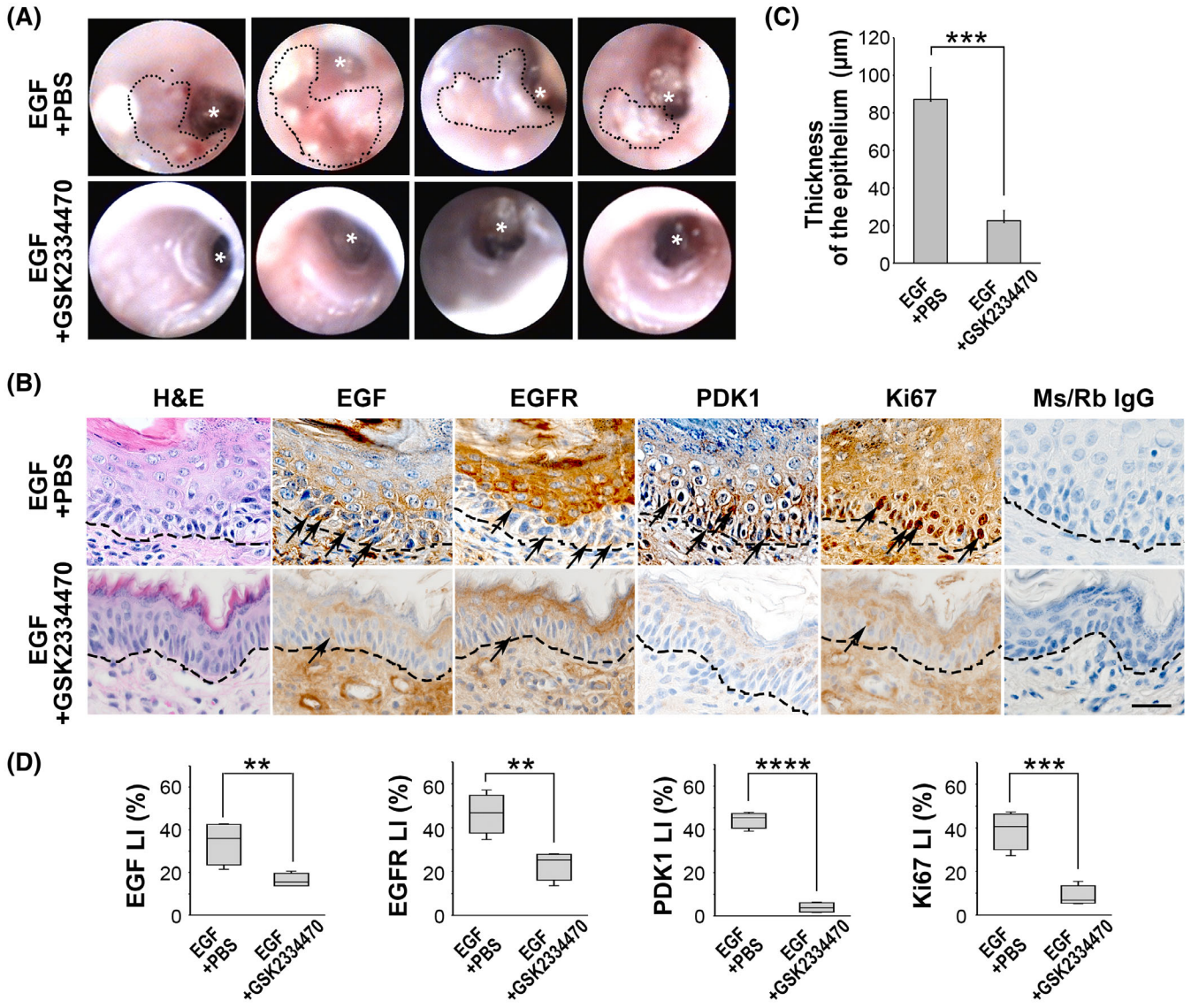

FIGURE 3 Effects of PDPK1 inhibitor (GSK2334470) against EGF-expression in the vector-transfected ears. (A) Otoendoscopic views of EGF-expression vector-transfected ears after PBS or GSK2334470 administration. The area within the dotted lines indicates the remains of protuberant tumor formation within the EAC in the PBS group, while tumor formation was not detected in the GSK2334470 group. (B) Morphological and immunohistochemical analysis. Hematoxylin and eosin (H&E) staining revealed a reduction of the thickened epithelium of the EAC in the GSK2334470 group, but thickened epithelium remained in the PBS group. Immunohistochemical analysis revealed the number of EGF-positive (+), EGFR+, PDPK1+, and Ki67+ cells was decreased in the GSK2334470 group as compared with the PBS group. Negative control was obtained by normal mouse (Ms) IgG and normal rabbit (Rb) IgG instead of first antibodies. (C) The bar graph shows the average of the epithelial thickness in the sections of the PBS group and the GSK2334470 group ($n = 4$ for each). (D) Labeling indexes (LIs) of EGF, EGFR, PDPK1, and Ki67 in the epithelium of the EAC in the PBS group versus in the GSK2334470 group ($n = 4$, each). Asterisks: tympanic membrane. Dashed lines: basement membrane. Arrows: positive cells. Scale bar: 20 μm. Error bars: 95% confidence interval. $^{**}p < .01$, $^{***}p < .001$, $^{****}p < .0001$

EGF-expression vector-transfected ears (4/4, 100%, data not shown), and it was indicated that EGF-expression vector was successfully transfected in the epithelial and subepithelial regions of the EAC. In the EGF-expression vector-transfected ears ($n = 4$, EGF group), the growth of a protuberant tumor was observed at the fifth transfection (4/4: 100%), whereas a normal appearance of the EAC and TM was observed in all of the ears in which empty vector was transfected (4/4: 100%) ($n = 4$, empty group) by otoendoscopic analysis (Figure 2A). Representative H&E staining of the EAC in the EGF group showed thickened epithelium as compared with the EAC in the PBS group (Figure 2B). An enzyme immunohistochemistry of EGF, EGFR, PDPK1, and Ki67 was performed in the empty group and EGF group (Figure 2B). According to the results, EGF+ cells and EGFR+ cells were observed in the lower layers of the EAC epithelium in the EGF group, whereas EGF+ and EGFR+ cells were scarcely found in the empty group (Figure 2B). PDPK1+ cells were also observed in the lower layers of the EAC epithelium in the EGF group,

but PDPK1+ cells were scarcely found in the empty group (Figure 2B). Ki67+ cells were increased in the EGF+/EGFR+/PDPK1+ layers of the EAC epithelium in the EGF group (Figure 2B). EGF LI of the EAC epithelial cells in the EGF group was significantly higher than in the empty group (39.2 ± 10.7 vs. 6.0 ± 1.1, p <.001, t-test, Figure 2C). EGFR LI was also higher in the EGF group than in the empty group (42.1 ± 4.7 vs. 8.8 ± 1.4, p <.0001, t-test, Figure 2C). Moreover, PDPK1 LI was significantly increased in the EGF group as compared with the empty group (43.3 ± 5.0 vs. 3.5 ± 1.4, p <.0001, t-test, Figure 2C). As expected, Ki67 LI of the EAC epithelium was also higher in the EGF group than in the empty group (45.0 ± 13.8 vs. 5.3 ± 1.8, p <.001, t-test, Figure 2C). These results indicated that the EGF-expression vector induced EGF- and EGFR-overexpression and led to PDPK1 upregulation. Moreover, PDPK1 upregulation led to an increase in cell proliferative activities in the EAC.

3.3 | Effects of GSK2334470 against EGF transfected ears

To assess the effects of PDPK1 inhibitor against EGF-expression in the vector-transfected ears, we administered the PDPK1 inhibitor GSK2334470 intraperitoneally ($n = 4$, GSK2334470 group), while PBS was used as the control ($n = 4$, PBS group). According to the results, a normal appearance of the EAC was observed in the GSK2334470 group as compared with the PBS group by otoendoscopic analysis (Figure 3A). H&E staining showed a notably reduced thickness of the epithelial region in the GSK2334470 group (Figure 3B), although a thickened epithelium remained in the PBS group (Figure 3B). The thickness of the epithelial region was significantly reduced in the GSK2334470 group as compared with the PBS group (22.7 ± 5.3 μm vs. 87.3 ± 17.0 μm, p <.001, t-test, Figure 3C). The number of PDPK1+ cells was decreased in the GSK2334470 group as compared with the PBS group immunohistochemically (Figure 3B). PDPK1 LI was significantly decreased in the GSK2334470 group as compared with the PBS group (44.4 ± 3.7 vs. 3.9 ± 2.2, p <.0001, t-test, Figure 3D). Ki67 LI was also reduced significantly in the GSK2334470 group (39.0 ± 8.7 vs. 8.6 ± 4.7, p <.001, t-test, Figure 3D). Interestingly, EGF and EGFR expression levels were also reduced in the GSK2334470 group as compared with the PBS group (Figure 3B), and EGF LI and EGFR LI were significantly reduced in the GSK2334470 group (34.0 ± 10.2 vs. 16.3 ± 3.2, p <.01, 46.4 ± 9.2 vs. 23.0 ± 6.6, p <.01, t-test, Figure 3D).

3.4 | GSK2334470 induced apoptosis in the EGF-expression vector-transfected ears

According to the results, we hypothesized that tumor regression by PDPK1 inhibition might be due to apoptosis. To assess this hypothesis, we analyzed apoptotic efficacy. As a result, TUNEL+ cells and cleaved caspase-3+ cells were increased both in the epithelial cells

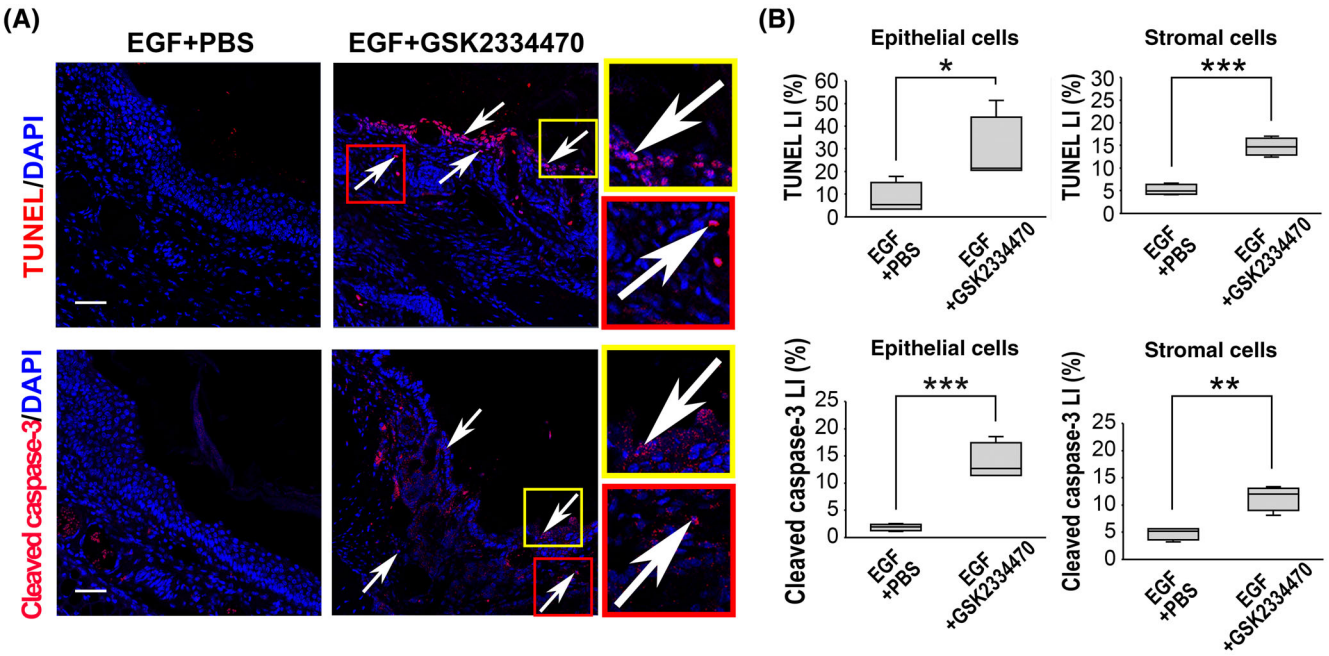

FIGURE 4 Apoptosis assay of the GSK2334470 effects against EGF-expression in the vector-transfected ears. (A) Terminal deoxy(d)-UTP nick end labeling (TUNEL) and immunofluorescent staining of cleaved caspase-3 of the EAC. GSK2334470 (GSK2334470 group, $n = 4$) or PBS (PBS group, $n = 4$) was administered intraperitoneally after EGF-expression vector transfection. TUNEL-positive (+) cells increased both in the epithelial cells and stromal cells. The number of TUNEL+ cells and cleaved caspase-3+ cells was increased in the epithelium and stroma in the GSK2334470 group as compared with the PBS group. Negative control was obtained by normal mouse (Ms) IgG and normal rabbit (Rb) IgG instead of the first antibodies. The nuclei were stained with DAPI (blue). (B) TUNEL labeling index (LI) and cleaved caspase-3 LI of the GSK2334470 group and the PBS group. The red- and yellow-boxed areas: higher magnification view. Arrows: positive cells. Scale bars: 50 μm. Error bars: 95% confidence interval. *p <.05, **p <.01, ***p <.001

and in the stromal cells in the GSK2334470 group as compared with the PBS group (Figure 4A). TUNEL LIs both in the epithelial cells and stromal cells increased significantly in the GSK2334470 group as compared with the PBS group (28.7 ± 15.1 vs. 8.0 ± 6.8, p <.05, 14.7 ± 1.9 vs. 5.2 ± 1.2, p <.001, t-test, Figure 4B). Cleaved caspase-3 LIs in both the epithelial cells and stromal cells also increased significantly in the GSK2334470 group (13.8 ± 3.4 vs. 1.9 ± 0.6, p <.001, 11.4 ± 2.3 vs. 4.8 ± 1.1, p <.01, t-test, Figure 4B). These results indicated that GSK2334470 induced an increase of apoptotic cells both in the epidermis and dermis of the EAC into which the EGF-expression vector was transfected.

4 | DISCUSSION

Activated EGFR is involved in the pathogenesis and progression of EACSCC the same as HNSCC,[10] but the pathogenesis of EACSCC is not fully understood. EACSCC is often accompanied by a marked inflammatory response and is suggested to be correlated with mechanical stimulations to the EAC.[36] In carcinoma tissues, the close correlation between chronic inflammation and a high risk of carcinogenesis has now been widely confirmed.[37] EGF acts in an autocrine and paracrine manner on their specific cell membrane receptor and mounts an effective reparative response to inflammatory change.[38] In this study, protuberant tumor formation and thickened epithelium were observed after the fifth transfection of the EGF-expression vector (4/4: 100%). We demonstrated EGFR LI was significantly increased in the EGF-expression vector-transfected ears compared with the empty vector-transfected ears immunohistochemically. These results indicated that EGFR overexpression was induced by transfection of the EGF-expression vector in the EAC.

PDPK1 plays an important role in tumor-cell growth downstream of the EGFR-mediated signaling pathways.[19–23] Expression of PDPK1 is higher in renal cell carcinoma,[39] bladder cancer,[40] prostate cancer,[41] lung cancer,[42] breast cancer,[41,43,44] hepatocellular carcinoma,[45] and HNSCC[21,23,46] compared with related normal tissues. In this study, it was confirmed that EGFR and PDPK1 were expressed in the human EACSCC specimens and colocalization was observed in the tumor region of the EAC immunohistochemically. Moreover, PDPK1 LI was significantly higher in the EGF-expression vector-transfected ears than in the empty vector-transfected ears in mice. As expected, Ki67+ cells were observed in the EGF+/EGFR+/PDPK1+ layers of the thickened epithelium in the EGF-expression vector-transfected ears and Ki67 LI was significantly increased. In other words, overexpression of EGFR and PDPK1 might play an important role in the proliferation of epithelial cells in the EAC into which the EGF-expression vector was transfected.

To confirm whether PDPK1 inhibition could reduce the EAC tumor induced by EGF overexpression, we conducted a PDPK1 inhibitory experiment against this animal model. We administered PDPK1 inhibitor GSK2334470 intraperitoneally in the EGF-overexpression model. As expected, the thickened squamous-cell layers of the EAC appeared normal by GSK2334470 administration. The number of PDPK1+ cells was apparently decreased and PDPK1 LI was significantly decreased in the GSK2334470 group compared with the PBS group. Moreover, Ki67 LI was significantly lower in the GSK2334470 group compared with the PBS group. These results indicated that systemic administration of GSK2334470 inhibited PDPK1 expression and induced tumor reduction effectively. In previous studies, it has been reported that PDPK1 inhibition induced apoptosis to suppress tumor formation in breast cancer and colorectal cancer.[43,47] To confirm apoptosis in the effects of GSK2334470 against EACSCC in this animal model, we performed a TUNEL assay and immunofluorescence staining using an anti-cleaved caspase-3 antibody. According to the results, TUNEL LIs both in the squamous cells and stromal cells were significantly increased in the GSK2334470 group. Interestingly, TUNEL+ cells were mainly observed in the outer layers of the squamous cells of the GSK2334470 group, whereas TUNEL+ cells were scarcely found in the PBS group. Cleaved caspase-3 LIs both in the epithelial cells and stromal cells were also significantly increased in the GSK2334470 group.

In conclusion, it is suggested that the EGFR/PDPK1 axis plays an important role in EACSCC, and the PDPK1 inhibitor, GSK2334470 could reduce the EACSCC inducing apoptosis. These results indicated that PDPK1 could be a therapeutic target of EACSCC and provide clinical benefits for patients in the future, although further investigation is required.

ACKNOWLEDGMENTS

We would like to thank Masahiro Takahashi, Kazuhisa Yamamoto, and Yutaka Yamamoto (Department of Otorhinolaryngology, Jikei University School of Medicine) for the harvesting of the human tissues; Hiroyuki Takahashi (Department of Pathology, Jikei University School of Medicine) for the pathological diagnosis; and Norifumi Tatsumi (Department of Anatomy, Jikei University School of Medicine) for his excellent technical assistance in this work. The authors alone are responsible for the content and writing of this article.

CONFLICT OF INTEREST

The authors report no conflicts of interest.

ORCID

Naotaro Akiyama https://orcid.org/0000-0002-2232-2049
Tomomi Yamamoto-Fukuda https://orcid.org/0000-0002-4168-6315
Hiromi Kojima https://orcid.org/0000-0003-2967-2110

REFERENCES

1. Brant JA, Eliades SJ, Chen J, Newman JG, Ruckenstein MJ. Carcinoma of the middle ear: a review of the national cancer database. *Otol Neurotol*. 2017;38(8):1153-1157.
2. Allanson BM, Low TH, Clark JR, Gupta R. Squamous cell carcinoma of the external auditory canal and temporal bone: an update. *Head Neck Pathol*. 2018;12(3):407-418.
3. Acharya PP, Sarma D, McKinnon B. Trends of temporal bone cancer: SEER database. *Am J Otolaryngol*. 2020;41(1):102297.
4. Nabuurs CH, Kievit W, Labbé N, et al. Evaluation of the modified Pittsburgh classification for predicting the disease-free survival

outcome of squamous cell carcinoma of the external auditory canal. *Head Neck*. 2020;42(12):3609-3622.
5. Sato K, Komune N, Hongo T, et al. Genetic landscape of external auditory canal squamous cell carcinoma. *Cancer Sci*. 2020;111(8):3010-3019.
6. Lechner M, Sutton L, Murkin C, et al. Squamous cell cancer of the temporal bone: a review of the literature. *Eur Arch Otorhinolaryngol*. 2021;278(7):2225-2228.
7. Makita K, Hamamoto Y, Takata N, et al. Prognostic significance of inflammatory response markers for locally advanced squamous cell carcinoma of the external auditory canal and middle ear. *J Radiat Res*. 2021;62(4):662-668.
8. Shinomiya H, Uehara N, Fujita T, et al. New proposal to revise the classification for squamous cell carcinoma of the external auditory canal and middle ear. *J Laryngol Otol*. 2021;135(4):297-303.
9. Normanno N, De Luca A, Bianco C, et al. Epidermal growth factor receptor (EGFR) signaling in cancer. *Gene*. 2006;366(1):2-16.
10. Maki D, Okami K, Ebisumoto K, et al. Immunohistochemical marker expression in temporal bone squamous cell carcinoma. *Tokai J Exp Clin Med*. 2021;46(2):89-93.
11. Basura GJ, Smith JD, Ellsperman S, Bhangale A, Brenner JC. Targeted molecular characterization of external auditory canal squamous cell carcinomas. *Laryngoscope Investig Otolaryngol*. 2021;6(5):1151-1157.
12. Morita S, Nakamaru Y, Homma A, et al. Expression of p53, p16, cyclin D1, epidermal growth factor receptor and Notch1 in patients with temporal bone squamous cell carcinoma. *Int J Clin Oncol*. 2017;22(1):181-189.
13. Kriegs M, Clauditz TS, Hoffer K, et al. Analyzing expression and phosphorylation of the EGF receptor in HNSCC. *Sci Rep*. 2019;9(1):13564.
14. Swaney DL, Ramms DJ, Wang Z, et al. A protein network map of head and neck cancer reveals PIK3CA mutant drug sensitivity. *Science*. 2021;374(6563):eabf2911.
15. Lu H, Lu Y, Xie Y, Qiu S, Li X, Fan Z. Rational combination with pyruvate dehydrogenase kinase 1 PDK1 inhibition overcomes cetuximab resistance in head and neck squamous cell carcinoma. *JCI Insight*. 2019;4(19):e131106.
16. Fasano M, Della Corte CM, Viscardi G, et al. Head and neck cancer: the role of anti-EGFR agents in the era of immunotherapy. *Ther Adv Med Oncol*. 2021;13:1758835920949418. doi:10.1177/1758835920949418. eCollection 2021.
17. Pollock NI, Grandis JR. HER2 as a therapeutic target in head and neck squamous cell carcinoma. *Clin Cancer Res*. 2015;21(3):526-533.
18. Ozawa H, Ranaweera RS, Izumchenko E, et al. SMAD4 loss is associated with cetuximab resistance and induction of MAPK/JNK activation in head and neck cancer cells. *Clin Cancer Res*. 2017;23(17):5162-5175.
19. Yarden Y, Sliwkowski MX. Untangling the ErbB signalling network. *Nat Rev Mol Cell Biol*. 2001;2(2):127-137.
20. Zhang Q, Thomas SM, Lui VW, et al. Phosphorylation of TNF-alpha converting enzyme by gastrin-releasing peptide induces amphiregulin release and EGF receptor activation. *Proc Natl Acad Sci U S A*. 2006;103(18):6901-6906.
21. Du L, Chen X, Cao Y, et al. Overexpression of PIK3CA in murine head and neck epithelium drives tumor invasion and metastasis through PDK1 and enhanced TGFβ signaling. *Oncogene*. 2016;35(35):4641-4652.
22. Ruicci KM, Plantinga P, Pinto N, et al. Disruption of the RICTOR/mTORC2 complex enhances the response of head and neck squamous cell carcinoma cells to PI3K inhibition. *Mol Oncol*. 2019;13(10):2160-2177.
23. Sambandam V, Frederick MJ, Shen L, et al. PDK1 mediates NOTCH1-mutated head and neck squamous carcinoma vulnerability to therapeutic PI3K/mTOR inhibition. *Clin Cancer Res*. 2019;25(11):3329-3340.
24. Yamamoto-Fukuda T, Aoki D, Hishikawa Y, Kobayashi T, Takahashi H, Koji T. Possible involvement of keratinocyte growth factor and its receptor in enhanced epithelial-cell proliferation and acquired recurrence of middle-ear cholesteatoma. *Lab Invest*. 2003;83(1):123-136.
25. Yamamoto-Fukuda T, Akiyama N, Shibata Y, Takahashi H, Ikeda T, Koji T. In vivo over-expression of KGF mimic human middle ear cholesteatoma. *Eur Arch Otorhinolaryngol*. 2015;272(10):2689-2696.
26. Yang C, Huang X, Liu H, et al. PDK1 inhibitor GSK2334470 exerts antitumor activity in multiple myeloma and forms a novel multi-targeted combination with dual mTORC1/C2 inhibitor PP242. *Oncotarget*. 2017;8(24):39185-39197.
27. Akiyama N, Yamamoto-Fukuda T, Yoshikawa M, Kojima H. Regulation of DNA methylation levels in the process of oral mucosal regeneration in a rat oral ulcer model. *Histol Histopathol*. 2020;35(3):247-256.
28. Yamamoto-Fukuda T, Akiyama N, Tatsumi N, Okabe M, Kojima H. Menin-MLL inhibitor blocks progression of middle ear cholesteatoma in vivo. *Int J Pediatr Otorhinolaryngol*. 2021;140:110545.
29. Akiyama N, Yamamoto-Fukuda T, Takahashi H. Influence of continuous negative pressure in the rat middle ear. *Laryngoscope*. 2014;124(10):2404-2410.
30. Akiyama N, Yamamoto-Fukuda T, Yoshikawa M, Kojima H. Evaluation of YAP signaling in a rat tympanic membrane under a continuous negative pressure load and in human middle ear cholesteatoma. *Acta Otolaryngol*. 2017;137(11):1158-1165.
31. Yamamoto-Fukuda T, Akiyama N, Takahashi M, Kojima H. Keratinocyte growth factor (KGF) modulates epidermal progenitor cell kinetics through activation of p63 in middle ear cholesteatoma. *J Assoc Res Otolaryngol*. 2018;19(3):223-241.
32. Yamamoto-Fukuda T, Akiyama N, Kojima H. Super-enhancer acquisition drives FOXC2 expression in middle ear cholesteatoma. *J Assoc Res Otolaryngol*. 2021;22(4):405-424.
33. Yamamoto-Fukuda T, Akiyama N, Kojima H. L1CAM-ILK-YAP mechanotransduction drives proliferative activity of epithelial cells in middle ear cholesteatoma. *Am J Pathol*. 2020;190(8):1667-1679.
34. Schneider CA, Rasband WS, Eliceiri KW. NIH Image to ImageJ: 25 years of image analysis. *Nat Methods*. 2012;9(7):671-675.
35. Thompson L. Update from the 4th Edition of the World Health Organization classification of head and neck tumours: tumours of the ear. *Head Neck Pathol*. 2017;11(1):78-87.
36. Tsunoda A, Sumi T, Terasaki O, Kishimoto S. Right dominance in the incidence of external auditory canal squamous cell carcinoma in the Japanese population: does handedness affect carcinogenesis? *Laryngoscope Investig Otolaryngol*. 2017;2(1):19-22.
37. Schäfer M, Werner S. Cancer as an overhealing wound: an old hypothesis revisited. *Nat Rev Mol Cell Biol*. 2008;9(8):628-638.
38. Pastore S, Mascia F, Mariani V, Girolomoni G. The epidermal growth factor receptor system in skin repair and inflammation. *J Invest Dermatol*. 2008;128(6):1365-1374.
39. Zhou WM, Wu GL, Huang J, et al. Low expression of PDK1 inhibits renal cell carcinoma cell proliferation, migration, invasion and epithelial mesenchymal transition through inhibition of the PI3K-PDPK1-Akt pathway. *Cell Signal*. 2019;56:1-14.
40. Kim CJ, Tambe Y, Mukaisho KI, et al. Periostin suppresses in vivo invasiveness via PDK1/Akt/mTOR signaling pathway in a mouse orthotopic model of bladder cancer. *Oncol Lett*. 2017;13(6):4276-4284.
41. Politz O, Siegel F, Bärfacker L, et al. BAY 1125976, a selective allosteric AKT1/2 inhibitor, exhibits high efficacy on AKT signaling-dependent tumor growth in mouse models. *Int J Cancer*. 2017;140(2):449-459.
42. Wang R, Zhang Q, Peng X, et al. Stellettin B induces G1 arrest, apoptosis and autophagy in human non-small cell lung cancer A549 cells via blocking PI3K/Akt/mTOR pathway. *Sci Rep*. 2016;6:27071.
43. Gagliardi PA, di Blasio L, Orso F, et al. 3-Phosphoinositide-dependent kinase 1 controls breast tumor growth in a kinase-dependent but Akt-independent manner. *Neoplasia*. 2012;14:719-731.
44. Fan R, Kim NG, Gumbiner BM. Regulation of Hippo pathway by mitogenic growth factors via phosphoinositide 3-kinase and phosphoinositide-dependent kinase-1. *Proc Natl Acad Sci U S A*. 2013;110(7):2569-2574.

45. Xia H, Dai X, Yu H, et al. EGFR-PI3K-PDK1 pathway regulates YAP signaling in hepatocellular carcinoma: the mechanism and its implications in targeted therapy. *Cell Death Dis*. 2018;9(3):269.
46. Jing P, Zhou S, Xu P, et al. PDK1 promotes metastasis by inducing epithelial–mesenchymal transition in hypopharyngeal carcinoma via the Notch1 signaling pathway. *Exp Cell Res*. 2020;386(2):111746.
47. Ericson K, Gan C, Cheong I, et al. Genetic inactivation of AKT1, AKT2, and PDPK1 in human colorectal cancer cells clarifies their roles in tumor growth regulation. *Proc Natl Acad Sci U S A*. 2010;107(6):2598-2603.

How to cite this article: Akiyama N, Yamamoto-Fukuda T, Yoshikawa M, Kojima H. Analysis of the epidermal growth factor receptor/phosphoinositide-dependent protein kinase-1 axis in tumor of the external auditory canal in response to epidermal growth factor stimulation. *Laryngoscope Investigative Otolaryngology*. 2022;7(3):730-739. doi:10.1002/lio2.785